OPEN ACCESS

University of BRISTOL

Peer reviewed version

Link to published version (if available):
10.2514/6.2015-1846

Link to publication record in Explore Bristol Research
PDF-document

Nonlinear Folding Wing-Tips for Gust Loads Alleviation

A. Castrichini[*]
Siemens PLM Software, Interleuvenlaan 68 Leuven, B-3001, Belgium

V. Hodigere Siddaramaiah[†], D.E. Calderon[†], J.E. Cooper[‡]
University of Bristol, Bristol, BS8 1TH, United Kingdom

T. Wilson[§]
Airbus Operations Ltd., Filton, BS99 7AR, United Kingdom

and
Y. Lemmens[**]
Siemens PLM Software, Interleuvenlaan 68 Leuven, B-3001, Belgium

A recent consideration in aircraft design is the use of folding wing-tips with the aim of enabling higher aspect ratio aircraft with less induced drag, but also meeting airport gate limitations. This study builds on previous work investigating the effect of exploiting folding wing-tips in-flight as a device to reduce dynamic gust loads, but now with the introduction of a passive nonlinear hinge spring to allow wing-tip deflections only for larger load cases. A representative civil jet aircraft aeroelastic model is used in a multi-body simulation code to explore the effect of introducing such a hinged wing-tip device on the loads behavior. It was found that significant reductions in the dynamic loads were possible.

Nomenclature

Symbols

b_l	=	Aerodynamic lag-pole	R_l	=	Aerodynamic states vector
c	=	Mean chord	$t_{release}$	=	Hinge moment threshold crossing time
D	=	Damping matrix	V	=	True air speed
D_θ	=	Hinge device damping	w	=	Gust vector
H	=	Gust gradient	w_g	=	Gust velocity
F_{Aero}	=	Aerodynamic forces vector	w_{g0}	=	Peak of the gust velocity
k	=	Reduced frequency	w_{ref}	=	Reference gust velocity
K	=	Stiffness matrix	x_0	=	Gust origin position
K_θ	=	Hinge device stiffness	x_j	=	j^{th} panel's control node position
L_g	=	Gust length	α	=	Angle of attack
q_{dyn}	=	Dynamic pressure	γ_j	=	j^{th} panel's dihedral angle
q_f	=	Modal coordinates	δ	=	Aerodynamic control surfaces vector
Q_0	=	Generalized aerodynamic force matrices	θ	=	Wing-tip folding angle
Q_e	=	External forces	Λ	=	Hinge orientation angle
Q_{i0}	=	Coefficient matrices of RFA	ξ	=	Generalized coordinates vector
Q_v	=	Quadratic velocity forces	Ψ	=	Body reference rotation
M_{Damp}	=	Hinge damping moment	*Superscript*		
M_{Max}	=	Hinge moment threshold value	$\cdot$	=	Differentiation with respect to time
			$\sim$	=	Fourier transform

[*] Research Engineer, Aerospace Competence Centre
[†] Postdoctoral Research Assistant, Department of Aerospace Engineering
[‡] Airbus Royal Academy of Engineering Sir George White Professor of Aerospace Engineering, Department of Aerospace Engineering, Associate Fellow AIAA
[§] Technical Competence Leader for Gust Loads & Aeroelastics, Flight Physics - Loads & Aeroelastics - EGLN
[**] Project Leader RTD, Aerospace Competence Centre

M_{NL}	=	Nonlinear hinge moment	$\bar{}$	=	Generalized variable
R	=	Body reference translation			

I. Introduction

Many efforts have been made in designing aircraft in order to optimize fuel consumption through reduction of aerodynamic drag. A sizable contribution to the global drag is lift-induced drag, which could be reduced by increasing the wingspan, but such a design solution has well defined limits imposed by the maximum aircraft dimensions allowed at airports. A possible solution to this problem is the use of folding wings that can be employed on the ground in a similar way to the retractable wings used on aircraft carrier borne aircraft. An example of this approach relevant to civil applications is the latest version of the B-777 which will have a folding wing capability to be activated during taxing to and from the gates. The inclusion of such a design feature raises the question as to whether such a folding device could also be used to enable loads reduction on the aircraft during the flight.

This work is aimed at studying the benefits of using a flexible wing-fold device for loads alleviation and considering how it would be implemented on civil jet aircraft. The main idea consists of introducing a hinge in order to allow the wing-tips (WT) to rotate, as shown in Fig. 1. The orientation of the hinge line relative to the direction of travel of the aircraft is a key parameter to enable successful loads alleviation [1]. When the hinge line is not along the $0°$ direction with respect the free stream, but is rotated outboard as in Fig. 1(b, d), folding the wing-tip then introduces a decrease in the local angle of attack. Knowing the hinge orientation Λ and the angle of rotation of the wing-tip θ, the variation of the local angle of attack $\Delta\alpha_{WT}$ can be shown to be given by

$$\Delta\alpha_{WT} = -\tan^{-1}(\tan\theta \sin\Lambda) \tag{1}$$

Such an effect implies that using a non $0°$ hinge angle provides a means to reduce the loads acting on the wing. It is thus expected that moderate hinge angles could lead to significant loads reductions, leading to the possibility of achieving a wing-tip extension with limited or even minimal impact on wing weight.
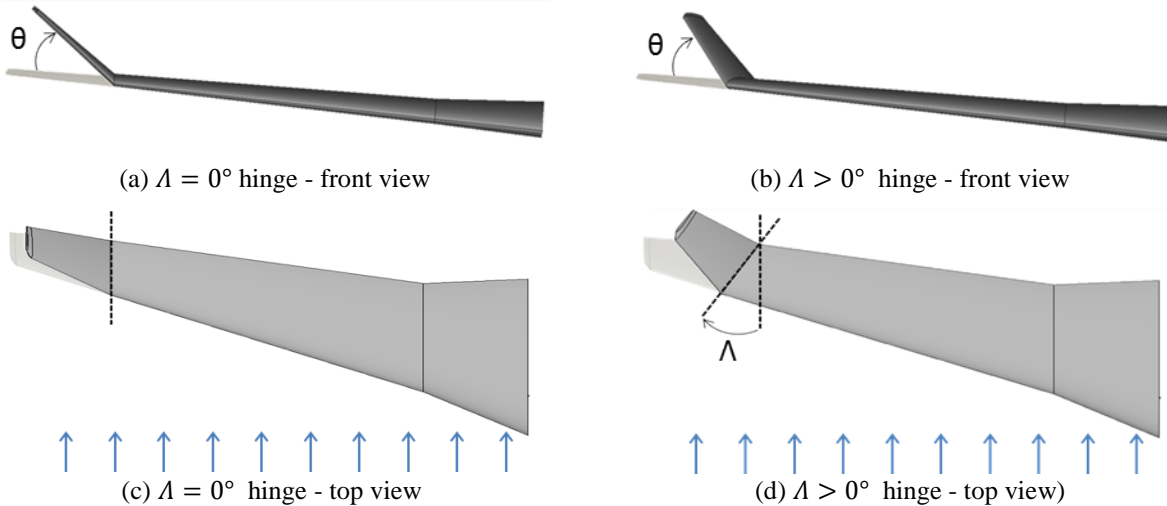

(a) $\Lambda = 0°$ hinge - front view	(b) $\Lambda > 0°$ hinge - front view
(c) $\Lambda = 0°$ hinge - top view	(d) $\Lambda > 0°$ hinge - top view)

Figure 1. Hinge Orientations

Previous work [1] considered several structural configurations for the loads alleviation device, varying the hinge direction, wing-tip weight, linear hinge spring stiffness and linear hinge damping value for static and dynamic gust loads. Figure 2 shows the aeroelastic model used for the analyses, which was a modified version of the FFAST aeroelastic model [2] of a representative civil jet aircraft, whose structure was modelled using a "stick" model with lumped masses and the aerodynamic forces determined using the doublet lattice panel method. The main objective was to investigate the possibility of having an aircraft configuration which enables a higher aspect ratio, in order to reduce the induced drag, by limiting the increase in loads (especially in terms of wing root bending moment) experienced by the aircraft, thus keeping the structure as light as possible. A baseline model, without wing-tips, in Fig. 2, was considered as the reference to evaluate the benefits or the disadvantages of using the folding wing-tips,

also shown in Fig. 2, which were attached to the structure using a flexible hinge, giving an increase in span of *25%* compared to the baseline. Figure 3 shows a detailed view of the structural model with the attached wing-tip device.

The hinge was modeled by constraining two coincident nodes, one belonging to the main airframe and the other to the wing-tip, to have the same translations but free to have different relative rotations with respect to a predefined hinge axis.
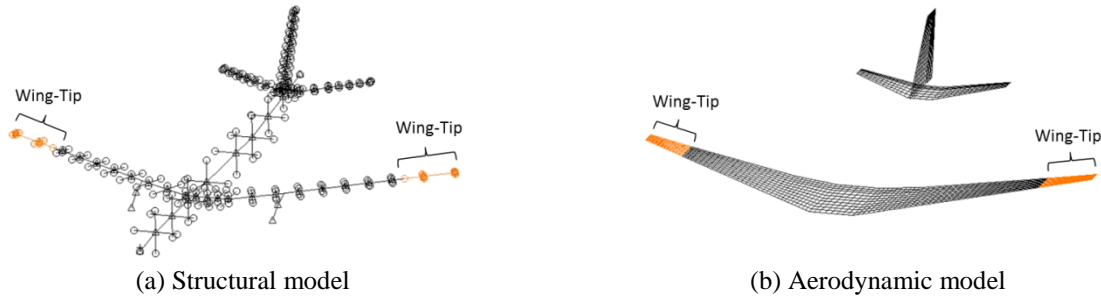

(a) Structural model   (b) Aerodynamic model

Figure 2. Aeroelastic Model Showing Baseline Model and Wing-Tips
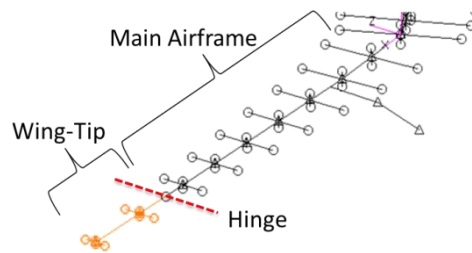

Figure 3. Folding Wing-Tip Modeling Detail

It was shown that a quick response of the wing-tip to the gust is essential for achieving an efficient loads reduction; the phase shift between the wing root bending moment (WRBM) and the folding angle should be as small as possible to let the wing-tip alleviate the loads. Significant reductions in the resulting loads were achieved with a passive linear hinge device for small hinge stiffness, no hinge damping, reduced wing-tip weight and swept hinge. Figure 4 shows the response of the linear commercial jet aircraft model to a *83 m* length gust for a baseline case and the same model but with a 25% wing-tip extension. The effect of including a *25°* hinge, a linear hinge spring with *1.E0 Nm/rad* stiffness, no hinge damping and a *100 Kg* wing-tip is illustrated. Figure 4(a) shows how the model with wing-tip extensions and flexible hinges (solid line) experienced gust increment loads (in this case wing root bending moment) close to those of the model with no extensions (dotted line), whereas the extended wing with a rigid hinge suffers much larger loads (dashed line). Examination of Fig. 4(b) shows that such a good load alleviation capability was achieved thanks to a negligible phase lag between the wing-tip deflection and the increment of the wing root bending moment; such a rapid deflection allowed the wing-tip to be mostly unloaded during the gust, as shown in Fig. 4(c). The inertial loads were small due to the low weight of the device and the wing-tip rotation produced negative aerodynamic forces that balanced the upward gust contribution. The use of a higher spring stiffness, hinge damping, or wing-tip mass induced a lower and slower wing-tip deflection with a consequent worsening of the loads alleviation capability [1].

However, having such a small hinge stiffness value leads the wing-tip to be deflected during straight and level cruise flight due to the static trim loads, and furthermore, to a continuous oscillating motion due to unsteady aerodynamic loads. Such deflections and continuous motions are undesirable as they will be detrimental to the aerodynamic performance, trim behavior and may generate undesired structural vibrations and rigid body motion. Ideally, the wing-tip should not deflect during cruise, but only operate once a significant gust is encountered. With a linear hinge device there is a conflict between having a low spring stiffness for good gust loads alleviation and a high spring stiffness to counteract static trim deflections and continuous oscillations. Consequently, a compromise in the design needs to be found in order to maximize the benefits of gust alleviation whilst avoiding motion during cruise which means that sub-optimal performance is achieved.

This paper builds upon the findings of the previous research work [1] regarding the analyses of static and dynamic gust responses for a linear hinge device. The same representative civil jet aircraft model is used, Fig. 2, but now an investigation is made into the use of a nonlinear hinge spring in order to activate the folding device only for

significant load cases, allowing wing-tip motion only when the aerodynamic loads are higher than some given threshold value.
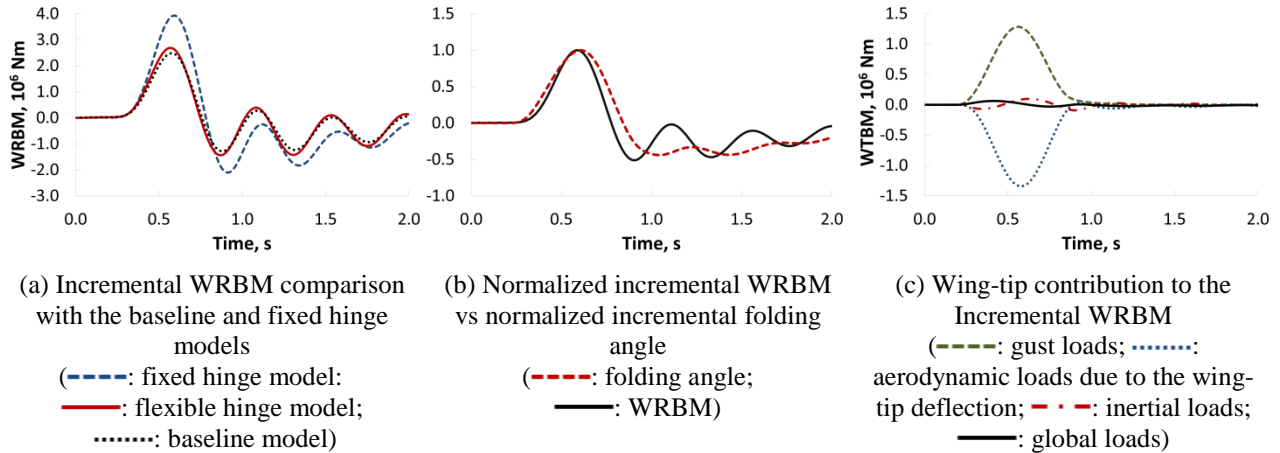

(a) Incremental WRBM comparison with the baseline and fixed hinge models
(━ ━ ━: fixed hinge model:
──: flexible hinge model;
········: baseline model)

(b) Normalized incremental WRBM vs normalized incremental folding angle
(━ ━ ━: folding angle;
──: WRBM)

(c) Wing-tip contribution to the Incremental WRBM
(━ ━ ━: gust loads; ········: aerodynamic loads due to the wing-tip deflection; ━ · ━: inertial loads; ──: global loads)

Figure 4. Linear Wing-Tip Model Gust Response ($L_g = 83\ m$)
($K_\theta = 1.\ Nm/rad, D_\theta = 0.\ Nms/rad, m = 100.\ Kg$)

II. Numerical Model

A. Structural Modeling

The commercial multibody code LMS Virtual.Lab Motion (VLM) was used for the aeroelastic analyses. The software enables nonlinear dynamic simulations of rigid and flexible multibody systems. Many formulations have been proposed in the literature to include the flexibility of a subcomponent in a multibody analysis, such as the floating frame of reference technique, the finite segment method, the finite element incremental method etc. [3] The floating frame of reference (FFR), is the formulation which has found the most widespread application and implementation in the commercial multibody packages, such as Virtual.Lab Motion. According the FFR formulation the configuration of a generic deformable body in the multibody system is identified by using two sets of coordinates: the reference coordinates which define the location R and orientation Ψ of a generic body reference, and the elastic coordinates q_f which describe the body local deformation with respect to the body reference by using linear dynamic condensation techniques such as Rayleigh-Ritz methods. Therefore, despite the multibody code allows the modelling of nonlinear finite translations and rotations for the body reference coordinates, the elastic coordinates, with the related modal shapes, can only describe small and linear deformations. The selected modal shapes have to satisfy the kinematic constraints imposed on the boundaries of the related deformable body due to the connection chain between the different subcomponents; therefore Craig-Bampton [4] mode sets are generally defined to take attachment effects into account.

The origin of the floating reference frame does not have to be rigidly attached to a material point on the deformable body, but it is required that there is no rigid body motion between the body and its coordinate system. This restriction means that the rigid body modes have to be removed from the modal basis used to describe the body deformation. The selection of the body reference is a key parameter for the correct formulation of the problem. For rigid body dynamics it is common to use centroidal body coordinates in order to decouple the inertial properties of rotational and translational degrees of freedom. However, the floating frame of reference formulation does not necessary lead to a separation between the rigid body motions and the elastic deformations, which may be coupled by the inertial properties of the body. This coupling strongly depends upon the choice of the floating frame of reference respect to which the modal shapes are defined. A weak inertial coupling could be achieved by using a mean-axis-frame, which requires using the eigenvectors of free-free structures [5]. With respect to the mean-axis-frame, the flexible modes do not induce any motion of the body center of gravity, thus allowing minimization of the kinetic energy related to the flexible modes, leading to a weak coupling between the reference motion and the elastic deformation [6].

The LMS Virtual.Lab Motion solver takes into account the effects due to the off-diagonal partitions of the mass matrix (often ignored), leading to the fundamental advantage of using multibody dynamics for aeroelastic

applications whereby there is a direct inertial coupling of flight mechanics and aeroelastic equations of motions on top of the usual aerodynamic coupling [7].

The mean-axis-frame enlarges also the applicability of the linearized equations for the flexible degrees of freedom since it is the reference with respect to which the deformations of the flexible body are minimized.

Aeroelastic simulations within the multibody package can be enabled through the definition of a user defined force element (UDF) to introduce linear aerodynamic forces into the system; however, a limitation that arises is that it is only possible to apply the aerodynamic forces to only one body of the multibody chain. The software has been formerly developed for the simulation of landing manoeuvers with the inclusion of aeroelastic and gusts loads, which required the application of the aerodynamic forces on the aircraft, but not on the landing gears. Therefore, for this work, it was not possible to split the main airframe and the two wing-tips as three separate entities, since all of them experience aerodynamic forces. Thus, only a single body was defined to model the entire assembly.

With such a modeling approach, the wing-tips deflection was enabled through the use of a specific set of modal shapes used to describe the flexibility of the overall assembly. The idea was to use the set of flexible modes obtained when a very low hinge spring stiffness was defined; a zero stiffness value was avoided to prevent numerical singularities during the modal analysis. This approach was implemented by setting the first two flexible modes as local symmetric and anti-symmetric pseudo-rigid wing-tips deflection as shown in Fig. 5(a, b). Such modal shapes are by definition orthogonal with the remaining flexible modes that involve a combination of wing-tips and main airframe deformations, Fig. 5(c, d), therefore they could be used to describe independent wing-tip rotations. It is important to point out that the wing-tip deflections were therefore modelled as linear local deformations and not as finite nonlinear rotations. The overall span reduction due to the wing-tips deflection was not considered.

Linear and nonlinear hinge devices, such as springs, dampers or actuators, can be modeled by applying external moments on the hinge nodes along the hinge axis in order to simulate the related restoring moments on the wing-tips and main airframe, as shown in Fig. 6. The hinge moments could be defined as linear or nonlinear functions of the wing-tip folding angle and, once projected onto the structural modes, defined as a set of generalized forces that could excite mainly the local wing-tip modes and so drive the wing-tips motion. The UDF capability was employed also to model the local hinge moments to be applied on the model. In this way it was possible to model local structural nonlinearities still using a set of linear normal modes to describe the dynamic response of the structure.

The numerical structural model used for these investigations, involved a *100 Kg* wing-tip model with a *25°* hinge and a hinge spring stiffness of *1.E0 Nm/rad*. Since a free flight condition was considered and no attachments effects between the airframe and the wing-tips were needed to be taken into account, a set of normal modes with free-free boundary conditions was so used to model the flexible airframe. A total of *44* flexible modes, up to *25. Hz*, were considered, with residual vectors also added to reduce the error due to modal truncation.
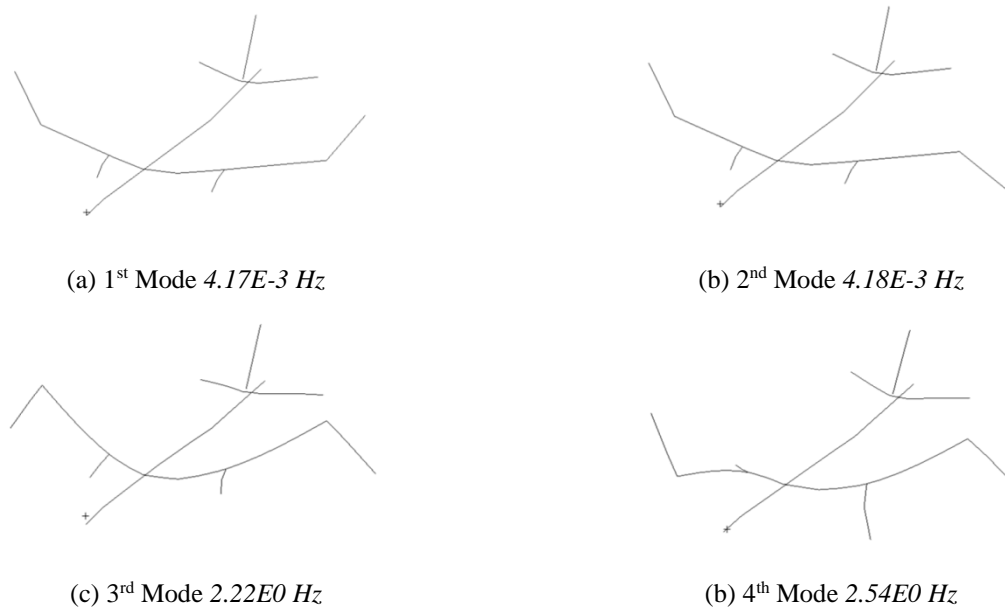

(a) 1st Mode *4.17E-3 Hz*

(b) 2nd Mode *4.18E-3 Hz*

(c) 3rd Mode *2.22E0 Hz*

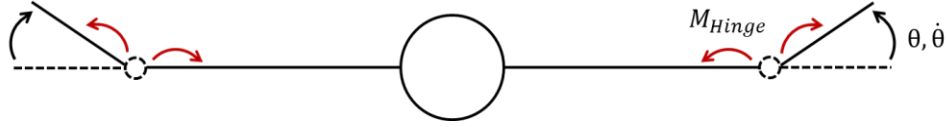(b) 4th Mode *2.54E0 Hz*

Figure 5. Lower Frequencies Structural Modes

Figure 6. Applied Hinge Moments

.The nonlinear dynamics equations of the system are described as

$$\bar{M}\ddot{\xi} + \bar{D}\dot{\xi} + \bar{K}\xi = \bar{Q}_v + \bar{Q}_e + \bar{F}_{Aero} + \bar{M}_{NL} + \bar{M}_{Damp}$$

$$
\begin{bmatrix} \bar{M}_{RR} & \bar{M}_{R\Psi} & \bar{M}_{Rf} \\ \bar{M}_{\Psi R} & \bar{M}_{\Psi\Psi} & \bar{M}_{\Psi f} \\ \bar{M}_{fr} & \bar{M}_{f\Psi} & \bar{M}_{ff} \end{bmatrix}
\begin{Bmatrix} \ddot{R} \\ \ddot{\Psi} \\ \ddot{q}_f \end{Bmatrix}
+ \begin{bmatrix} 0 & 0 & 0 \\ 0 & 0 & 0 \\ 0 & 0 & \bar{D}_{ff} \end{bmatrix}
\begin{Bmatrix} \dot{R} \\ \dot{\Psi} \\ \dot{q}_f \end{Bmatrix}
+ \begin{bmatrix} 0 & 0 & 0 \\ 0 & 0 & 0 \\ 0 & 0 & \bar{K}_{ff} \end{bmatrix}
\begin{Bmatrix} R \\ \Psi \\ q_f \end{Bmatrix}
$$

$$
= \begin{Bmatrix} \bar{Q}_{vR} \\ \bar{Q}_{v\Psi} \\ \bar{Q}_{vf} \end{Bmatrix}
+ \begin{Bmatrix} \bar{Q}_{eR} \\ \bar{Q}_{e\Psi} \\ \bar{Q}_{ef} \end{Bmatrix}
+ \begin{Bmatrix} \bar{F}_{Aero\,R} \\ \bar{F}_{Aero\,\Psi} \\ \bar{F}_{Aero\,f} \end{Bmatrix}
+ \begin{Bmatrix} 0 \\ 0 \\ \bar{M}_{NL}(q_f)_f \end{Bmatrix}
+ \begin{Bmatrix} 0 \\ 0 \\ \bar{M}_{Damp}(q_f)_f \end{Bmatrix}
\tag{2}
$$

where ξ is the vector of the generalized coordinates of the body which includes the rigid body translations $\{R_1, R_2, R_3\}$ and rotations $\{\Psi_1, \Psi_2, \Psi_3\}$ and the modal elastic coordinates $\{q_{f1}, \dots q_{fN_{Modes}}\}$ related to the linear flexible modes as shown in Fig. 5, $\bar{M}, \bar{D}, \bar{K}$ are the generalized mass, damping and stiffness matrices respectively, $\bar{Q}_v$ are the quadratic velocity forces (Coriolis and centrifugal terms), $\bar{Q}_e$ are the generalized external forces, in this case, due to gravity, $\bar{F}_{Aero}$ are the generalized aerodynamic forces, $\bar{M}_{NL}$ are the generalized moments due to the hinge nonlinear spring and $\bar{M}_{Damp}$ are the generalized moments due to the hinge damping element.

The idea was to simulate a mechanism that allowed the wing-tip to rotate only when the aerodynamic forces generated a hinge moment higher than some predefined threshold value M_{max}. Such device was modeled by applying, to the wing-tips and main airframe, the restoring moments due to a piecewise linear spring whose stiffness was varied according the loads experienced by the aircraft such that

$$M_{NL} = -K_\theta \theta$$
$$
\begin{cases}
K_\theta = 1.E^{12} Nm/rad & if \quad K_\theta \theta \leq M_{max} \ and \ 0 < t < t_{release} \\
K_\theta = 1.E^{0} Nm/rad & if \quad K_\theta \theta > M_{max} \ and \ t \geq t_{release}
\end{cases}
\tag{3}
$$

The hinge moment due to a linear hinge damping element was defined as

$$M_{Damp} = -D_\theta \dot{\theta} \tag{4}$$

It is expected that, once released, the wing-tips would fold up, pushed both by the dynamic gust and the static trim loads. The latter, formerly balanced by the high spring stiffness, would continue to provide a hinge moment even after the gust event leading the wing-tip to remain deflected, unless there was some way of trimming the wing-tip in cruise.

The external hinge moments, defined in Eqs. (3) and (4) were projected onto the modal basis in order to evaluate the related generalized moments to be applied on the flexible body.

B. Aerodynamic Modeling

The doublet lattice method [8,9] was employed to model the aerodynamic forces which, in the frequency domain, are defined as

$$F_{Aero} = q_{dyn}[Q\tilde{\xi} + Q_x\tilde{\delta} + Q_g\tilde{w}] \tag{5}$$

where $Q_{(N_{Modes}+6\ X\ N_{Modes}+6)}$, $Q_{x(N_{Modes}+6\ X\ N_{ControlSurf})}$ and $Q_{g(N_{Modes}+6\ X\ N_{Panels})}$ are respectively the generalized aerodynamic forces matrices related to the Fourier transform of the generalized coordinates $\tilde{\xi}$, control surfaces vector $\tilde{\delta}$ and gust vector $\tilde{w}$.

Only the aircraft longitudinal dynamics were of interest for this work, therefore δ is a scalar variable representing the elevator deflection. Employing a nonlinear structural model meant that the dynamic gust responses had to be computed from a trimmed flight configuration, since the superimposition of the static and dynamic responses was no longer feasible. The control of the aircraft motion was achieved by running in parallel the multibody code and Matlab-Simulink. The rigid body displacements and velocities were measured and sent to Matlab-Simulink where PID controls were used to evaluate the elevator deflection, which was then passed back to the UDF to generate the related aerodynamic forces for application to the aircraft. Such a framework could be used to perform a wide range of manoeuvers such as static trim, pull-up, roll etc., whether more control surfaces (aileron, rudder…) were defined. Given that no physical control surfaces were defined on structural model, as showed in Fig. 2(a), the aerodynamic forces due to the elevator deflection were evaluated by means of transpiration boundary conditions, i.e. by applying a local variation of the downwash velocity on the elevator's aerodynamic panels without actually rotate it.

The gust vector defines the downwash on a generic aerodynamic panel j due to the gust such that

$$w_j = \cos\gamma_j \frac{w_{g0}}{2V}\left(1 - \cos\left(\frac{2\pi V}{L_g}\left(t - \frac{x_0 - x_j}{V}\right)\right)\right) \tag{6}$$

where γ_j is the dihedral angle of the jth panel, $x_0 - x_j$ is the distance of the jth panel with respect the gust origin, L_g is the gust length (twice the gust gradient H), V is the true air speed and w_{g0} peak gust velocity. The latter defined (in m) as [10]

$$w_{g0} = w_{ref}\left(\frac{H}{106.17}\right)^{\frac{1}{6}} \tag{7}$$

The aerodynamic matrices Q, Q_x, Q_g were computed for a limited number of reduced frequencies $\left(k = \frac{\omega c}{2V}\right)$ and at a given Mach number. In order to allow for simulation in the time domain, the aerodynamic matrices were approximated, in the frequency domain, using the rational fraction approximation (RFA) method proposed by Roger [11]. Following some manipulation, the aerodynamic loads can be formulated in the time domain as

$$F_{Aero} = q_{dyn}\left\{\left[Q_0\xi + \frac{c}{2V}Q_1\dot\xi + \left(\frac{c}{2V}\right)^2 Q_2\ddot\xi\right] + \left[Q_{x0}\delta + \frac{c}{2V}Q_{x1}\dot\delta + \left(\frac{c}{2V}\right)^2 Q_{x2}\ddot\delta\right]\right.$$
$$\left. + \left[Q_{g0}w + \frac{c}{2V}Q_{g1}\dot w + \left(\frac{c}{2V}\right)^2 Q_{g2}\ddot w\right] + \sum_{l=1}^{N_{Poles}} R_l\right\} \tag{8}$$

where R_l is the generic aerodynamic state vector related to the generic lag-pole $b_l = \frac{k_{max}}{l}$. These extra states allowed the modeling of the unsteady response of the aerodynamics by taking into account of the delay of the aerodynamic forces with respect to the structural deformations. These aerodynamic states were evaluated through the set of dynamic equations

$$\dot R_l = -b_l \frac{2V}{c}IR_l + Q_{2+l}\dot\xi + Q_{x2+l}\dot\delta + Q_{g2+l}\dot w \qquad l = 1, …, N_{Poles} \tag{9}$$

which were written in the UDF environment and solved using the LMS Virtual.Lab Motion solver together with the equations of motion.

Several authors [12,13] have handled the coupling of rigid body flight dynamics and aeroelastic models by using CFD models or experimental aerodynamic data to describe the aerodynamic forces due to the rigid body motion. However, for this work, the double lattice method was employed to define the rigid body forces as well. The free-free structural modes were calculated using the Givens method in order to have rigid body modes that represented

translations and rotations around the center of gravity of the aircraft. These modes were scaled to involve unit translations and rotations so that the aerodynamic generalized forces related to the rigid body modes were coherent with the rigid body generalized coordinates of the LMS Virtual.Lab Motion model.

It was found that the rigid body forces were particularly sensitive to the stiffness and damping terms of the related aerodynamic forces, a small error on their evaluation could lead the solution to diverge after the gust event. A solution was found by defining a hybrid rational fraction approximation of the aerodynamic matrix Q as shown in Fig. 7; an unsteady formulation, with 5 extra aerodynamic poles and a maximum reduced frequency of $k_{max}=1.$, for the flexible modes columns ($7, ..., N_{Modes}$); a quasi-steady formulation, with no aerodynamic poles and a maximum reduced frequency of $k_{max}=0.01$, for the terms related of the rigid body modes columns ($1, ..., 6$). The latter was acceptable due to the low frequency range of the rigid body degrees of freedom and ensured a more accurate modeling of their related aerodynamic stiffness and damping forces terms.

Equations (5) and (6) show that the gust was not modeled as a single scalar value, but as vector of gusts defined for each aerodynamic panel. Each component of the gust vector w was delayed in time in function of the position of the related panel with respect the origin of the gust. Although this approach leads to bigger Q_g matrices, it does enable a more accurate approximation of the aerodynamic gust matrix terms; the modeling of the delay directly in the time domain and not in the frequency, has prevented the typical spiral trend which in general affects the gust terms and that is poorly approximated when a restricted number of extra aerodynamic poles are used.

III.   Results

The dynamic gust response analyses were performed starting from the trimmed flight configuration. A "1-g" load case was considered with the aircraft operating at $M=0.6$ at $25,000\,ft$, equivalent to a dynamic pressure of $9.47KPa$. Several gust response analyses were then made over a range of gust lengths for a given flight configuration; with reference to Eq. (7), w_{ref} was varied linearly from $13.4\,m/s$ EAS at $15,000\,ft$ to $7.9\,m/s$ EAS at $50,000\,ft$, based on FAA Federal Aviation and EASA Regulations. At the investigated flight altitude of $25,000\,ft$ and Mach number of 0.6, the gust reference velocity was $11.48\,m/s$ EAS, while the gust lengths varied between $18\,m$ and $214\,m$ [10].

(a) $Q[3,3], k_{max} = 0.01$ (b) $Q[3,7], k_{max} = 1.$ (c) $Q[5,7], k_{max} = 1.$

(d) $Q[5,5], k_{max} = 0.01$ (e) $Q[35,37], k_{max} = 1.$ (f) $Q[9,9], k_{max} = 1.$
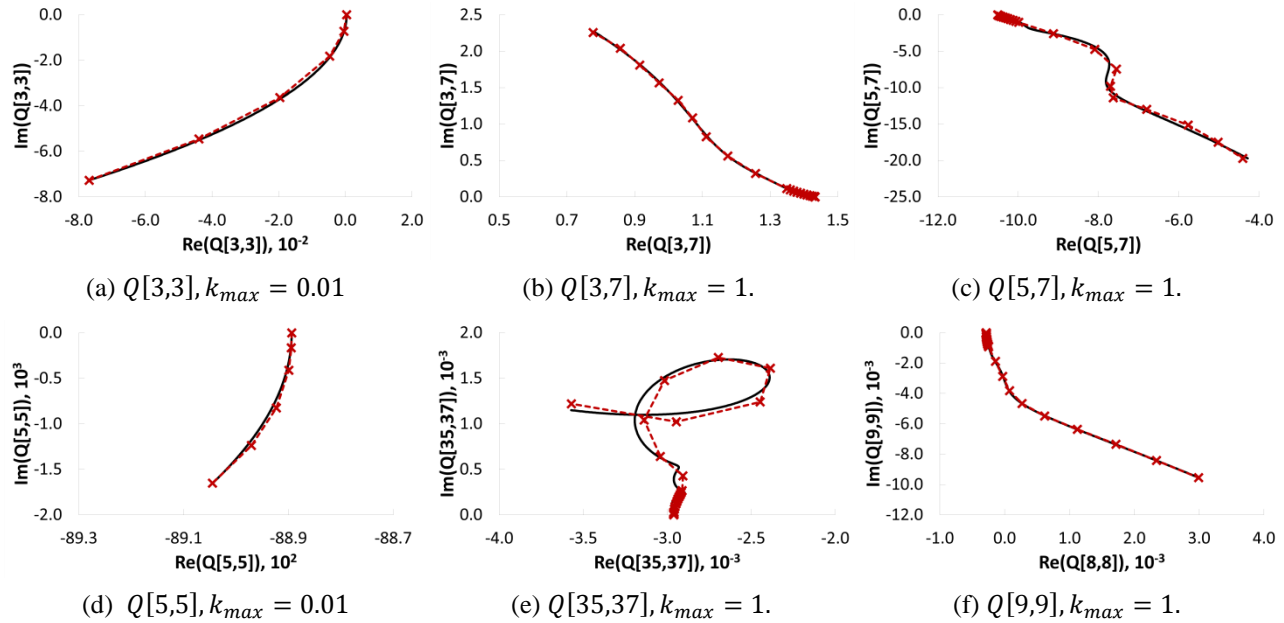
Figure 7. Hybrid RFA of the Generalized Aerodynamic Matrix Q
(——✱——: Nastran; ———: RFA)

A. Multibody Aeroelastic Model Validation

The validation of the LMS Virtual.Lab Motion model and the related UDF was achieved by comparing the results of several gust analyses with those obtained using an equivalent Nastran model. A linear spring was defined on the structural hinge, as in Eq. (3), but with the stiffness remaining constant during the simulation. Several gusts

lengths and spring stiffness values were considered. No trim analysis was performed, and only the incremental gust loads were applied on the structure.

For all of the investigated configurations, the equivalent restoring moments, applied on the hinge of the LMS Virtual.Lab Motion model, proved to correctly model the effect due to a linear hinge spring. With regard to the modeling of the aerodynamics, the time domain formulation of the aerodynamic matrices showed a very good approximation of the doublet lattice aerodynamic forces over a set of gust lengths and thus for different range of reduced frequencies. Figure 8 shows that there was a very good correspondence between the Nastran and the LMS Virtual.Lab Motion gust responses both in terms of incremental wing root bending moment and global wing-tip vertical displacement.
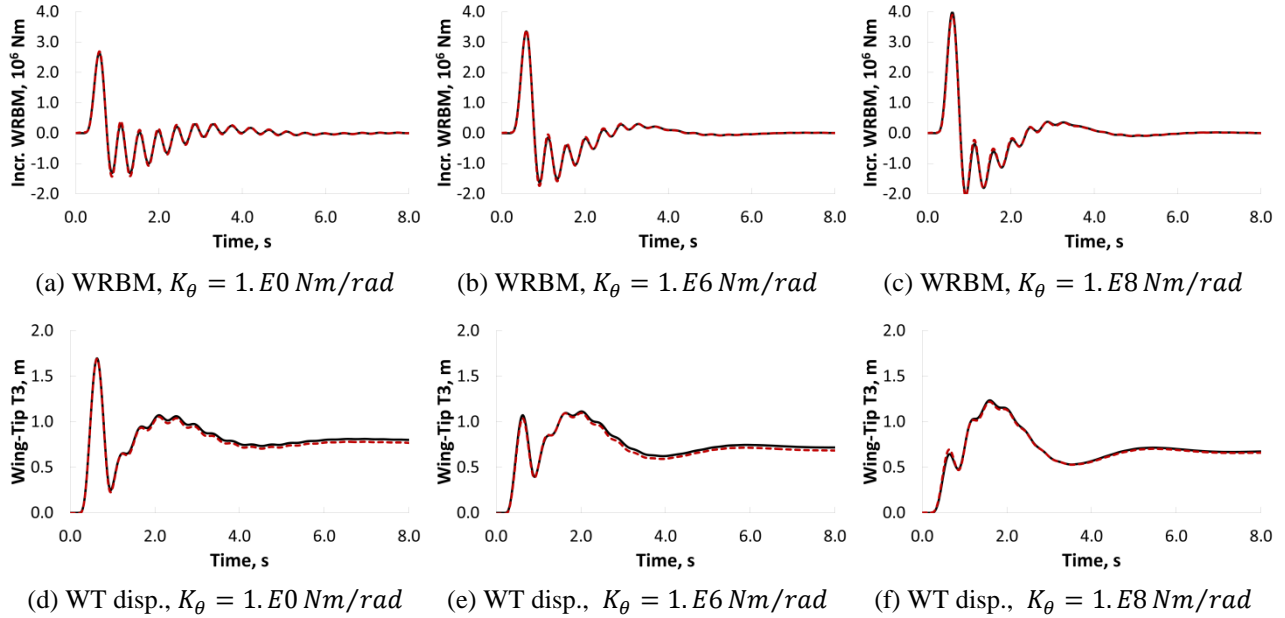

(a) WRBM, $K_\theta = 1.E0\ Nm/rad$ (b) WRBM, $K_\theta = 1.E6\ Nm/rad$ (c) WRBM, $K_\theta = 1.E8\ Nm/rad$

(d) WT disp., $K_\theta = 1.E0\ Nm/rad$ (e) WT disp., $K_\theta = 1.E6\ Nm/rad$ (f) WT disp., $K_\theta = 1.E8\ Nm/rad$

Figure 8. VLM vs Nastran Gust Response (Lg=127m)
(━━: VLM, ----: Nastran)

B. Aeroelastic Trim

Figures 9 and 10 show the results of the aeroelastic trim analysis in terms of structural deformation, trim angle of attack, *6.25 deg*, and elevator deflection, *-12.39 deg*. For the trim analyses a fixed hinge model was employed by defining a linear torsional spring of *1.E12 Nm/rad*. From the trim analysis it was found that, for the given trim flight condition, the aerodynamic forces provided a static hinge moment of around *2.70E5 Nm*, such value was considered as a reference for the definition of the hinge moment threshold values for the nonlinear spring modeling. The convergence to a steady trimmed flight configuration was enhanced by defining higher values for the structural and aerodynamic damping with respect to those considered in the following gust analyses.

An equivalent Nastran static trim analysis was also performed as further validation of the multibody aeroelastic model; the analyses presented a very good match in term of trim angle of attack and elevator deflection.
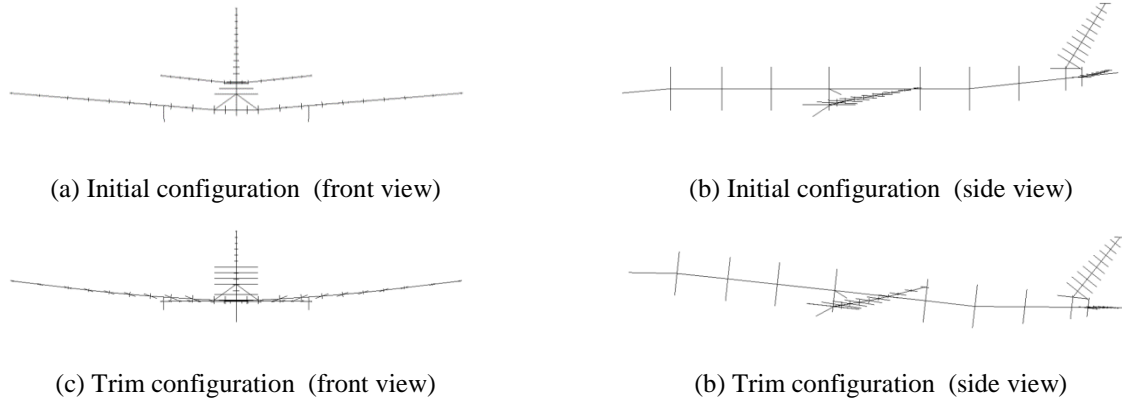
(a) Initial configuration (front view)

(b) Initial configuration (side view)

(c) Trim configuration (front view)

(b) Trim configuration (side view)

Figure 9. Static Trim Deformation
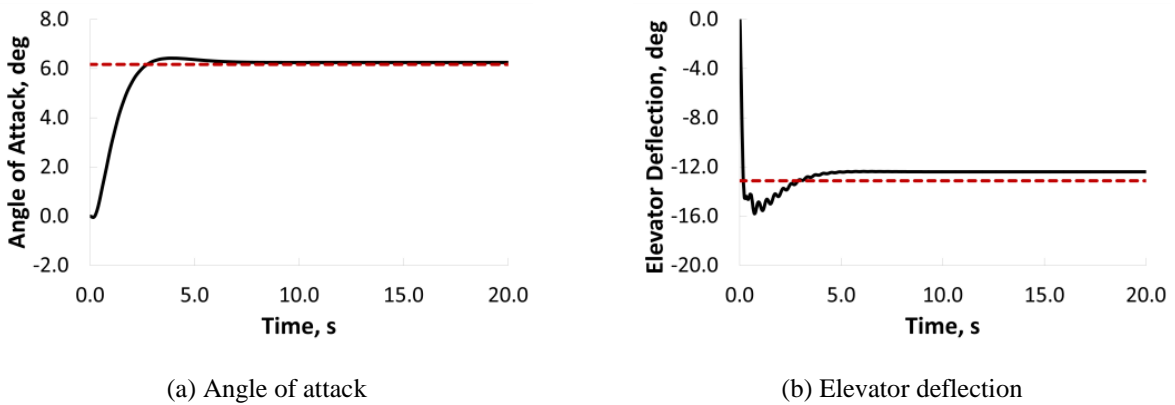

(a) Angle of attack

(b) Elevator deflection

Figure 10. Trim Elevator and Angle of Attack
(———: VLM, ----: Nastran)

C. Nonlinear Gust Response

The dynamic gust response of the model with a nonlinear folding device was then considered. The wing-tip rotation was only allowed to occur when the aerodynamic forces generated a hinge moment higher than some pre-defined value. Once released, the wing-tip folding device reacted as a linear spring with $1.E0\ Nm/rad$ of stiffness, so the nonlinear spring behaved as a piecewise linear spring. Figure 11 shows the hinge moments over a range of gust lengths for the fixed hinge model, where $3.0E5\ Nm$, $3.3E5\ Nm$ and $3.6E5\ Nm$ were considered as threshold values for the reduction hinge spring stiffness. Different damping values for the hinge device were also considered.
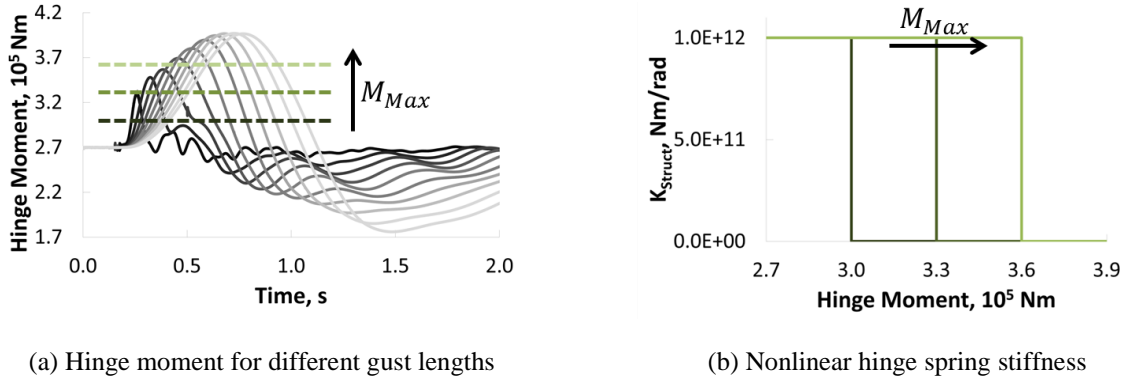

(a) Hinge moment for different gust lengths

(b) Nonlinear hinge spring stiffness

Figure 11. Hinge Moments Threshold Values and Spring Stiffness

Figure 12 shows the envelope of the maximum and minimum incremental wing root bending moments (with respect to the trimmed flight configuration) over a range of gust lengths for different hinge moment threshold and hinge damping values. The wing root bending moment and wing-tip deflection time histories for the same structural configurations and a gust length of *83 m* are shown in Fig. 13.

When the hinge stiffness was reduced from *1.E12 Nm/rad* to *1.E0 Nm/rad* and small hinge damping values were employed, $D_\theta \leq 1.E5 Nms/rad$, the wing-tips folded up driven by the positive static trim and dynamic gust loads, the combination of these two contributions allowed the folding device to rotate quickly leading to a good reduction of the positive gust loads. For a small hinge moment threshold, *3.0E5 Nm*, and hinge damping values of *0. Nms/rad* and *1.E5 Nms/rad*, the incremental positive gust loads were even lower with respect those of the baseline model. As might be expected, the higher the threshold value, the later the wing-tip started to rotate, producing a delay in the folding device's response, as shown in Figs. 13(b, d, f), leading to a worse alleviation capability on the maximum experienced load, due to the reduced time available to counter the gust. The minimum loads were instead always lower than those from the fixed hinge model as the static trim loads provided a positive hinge moment that did not allow to the wing-tip to fold downwards, Figs. 13(b, d, f). The wing-tip could generate only a negative lift contribution leading to an increment of the minimum loads. Nevertheless structural sizing and loads assessment require the combination of the positive static trim loads with the incremental gust ones, as consequence the positive gust loads, which were reduced by the wing-tip device, result to be the most critical for the structure.
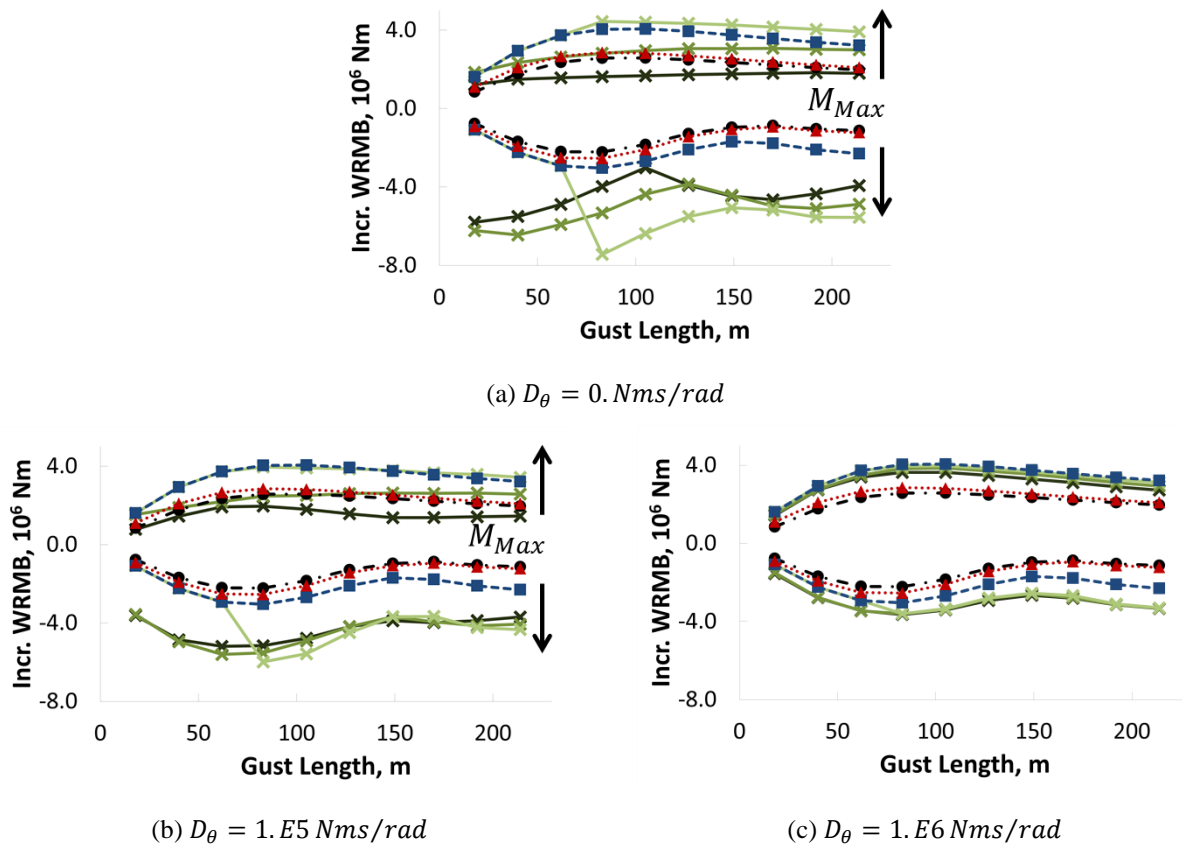

(a) $D_\theta = 0. Nms/rad$

(b) $D_\theta = 1. E5 Nms/rad$

(c) $D_\theta = 1. E6 Nms/rad$

Figure 12. WRBM Envelopes for Different Hinge Moments Threshold and Hinge Damping Values (Lg=83m)
(- ■ -:fixed hinge model; - ● -:baseline model; ···▲···:linear model $K_\theta = 1. E0 Nm/rad$ and $D_\theta = 0. Nms/rad$; ✱:nonlinear model $M_{max} = [3. 0E05, 3. 3E05, 3. 6E05] Nm$)

Although, from an aerodynamic point of view, a fast wing-tip rotation is essential for achieving good loads alleviation allowing a quick reduction wing-tip lift, the inertial loads need also to be taken into account. For a given wing-tip mass, the faster the initial wing-tip rotation, the greater the inertial force as the maximum rotation angle is approached. From Fig. 13(b) it can be seen how, when no hinge damping element was defined, the wing-tip

experienced a very fast rotation moving from *0°* to *40°* , leading to a positive peak of the wing root bending moment due to the wing-tip inertial loads, Fig. 13(a). When the threshold value was *3.6E5 Nm*, this effect led to loads higher than the ones of the fixed hinge model. The introduction of hinge damping element is beneficial as this reduces the initial inertial loads contribution; however, the higher the damping, the slower the wing-tip rotation, thus worsening the loads alleviation capability. Figure 13(c) show how a damping value of *1.E5 Nms/rad* was found to be a good compromise, leading to the reduction of the inertial peaks without jeopardizing the generation of the wing-tip negative lift contribution.
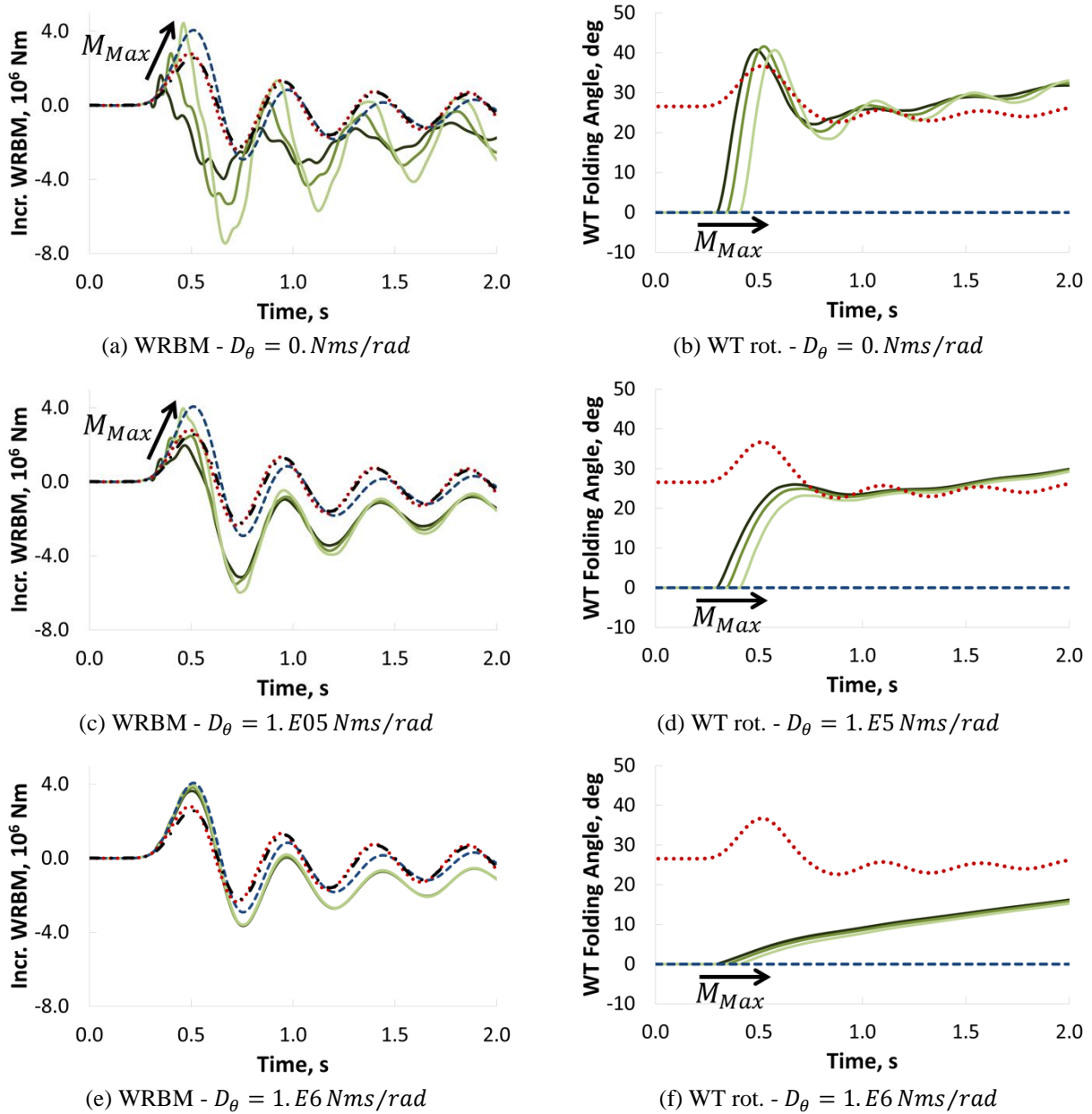

(a) WRBM - $D_\theta = 0. Nms/rad$ (b) WT rot. - $D_\theta = 0. Nms/rad$

(c) WRBM - $D_\theta = 1.E05 Nms/rad$ (d) WT rot. - $D_\theta = 1.E5 Nms/rad$

(e) WRBM - $D_\theta = 1.E6 Nms/rad$ (f) WT rot. - $D_\theta = 1.E6 Nms/rad$

Figure 13. Wing-Tip Dynamic Response for Different Hinge Moments Threshold and Hinge Damping Values (Lg=83m)
(– – – –:fixed hinge model; – · –:baseline model; ·······:linear model $K_\theta = 1.E0 Nm/rad$ and $D_\theta = 0. Nms/rad$; ——:nonlinear model $M_{max} = [3.0E05, 3.3E05, 3.6E05] Nm$)

Figure 14 shows the generic steady deformation and flight configuration of the aircraft after the gust encounter and the reduction of the hinge stiffness from *1.E12 Nm/rad* to *1.E0 Nm/rad*. In Fig. 15 it can be seen that the steady

values of the incremental wing root bending moments are *-1.05E6 Nm*, with a wing-tip folding angle of *31.81°*, for all different hinge moment threshold and hinge damping values combinations considered. The aircraft steady response is only function of the angle of attack, elevator deflection and dynamic pressure and does not depend upon on the hinge moment threshold or hinge damping values defined for the hinge device. The negative value for the steady incremental wing root bending moment is due to the incremental loads being defined with respect the fixed hinge trim configuration; the wing-tips, when folded, generate a negative contribution to the wing root bending moment.

| (a) front view | (b) side view |

Figure 14. Aircraft Steady Response After the Gust Transient

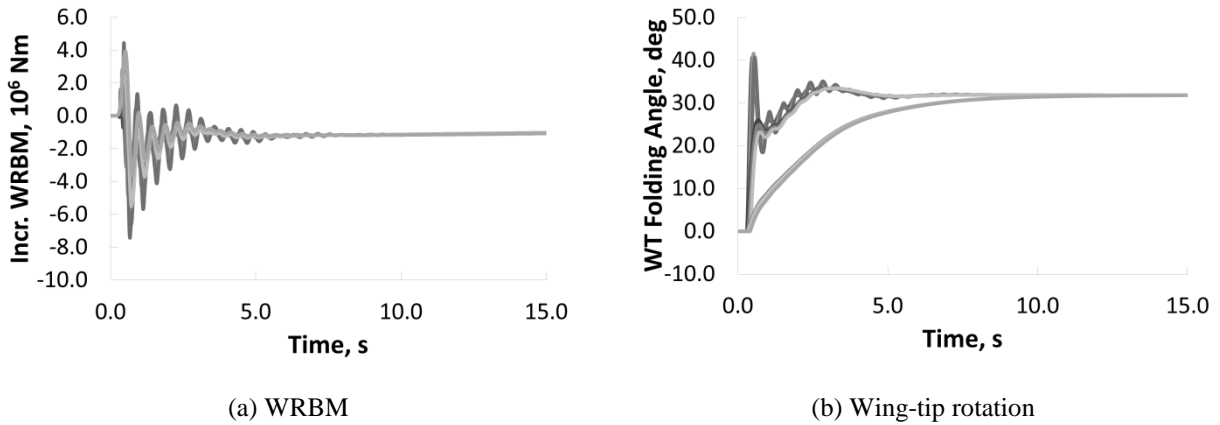| (a) WRBM | (b) Wing-tip rotation |

Figure 15. Steady WRBMs and Wing-Tip Deflections After the Gust Transient

IV.   Conclusions

A preliminary investigation on the use of nonlinear folding wing-tips as a loads alleviation device was performed using a numerical aeroelastic model of a typical commercial jet aircraft. A wing-tip device was connected to the wings with a hinge, and the effects of a nonlinear hinge device, on "1-cosine" gusts, were investigated. All results were related to the loads acting on a baseline model which consisted of the aircraft without wing-tips i.e. *20%* less span.

The nonlinear hinge device was employed in order to only implement the device in extreme loading levels via a piecewise linear stiffness; the results have highlighted that the loads alleviation capabilities were strongly affected by the hinge moment threshold to the release of the wing-tip and by the hinge damping value. Low threshold of moments combined with low hinge damping allowed a rapid deflection of the folding device, driven by the positive gust and trim loads, leading to incremental wing root bending moment even lower than those of the baseline model.

A non-zero hinge damping value was beneficial, allowing the reduction of the inertial loads due to the fast wing-tip rotation, while too high a value is to be avoided since an overdamped system worsens the loads alleviation.
It was shown that increasing the hinge moment threshold of the nonlinear device delayed the onset of the wing-tip rotation and led to higher wing root bending moments.

The limit of the presented loads alleviation strategy as described is that, once released, the wing-tips would remain deflected even after the gust event because of the positive static trim loads. Some form of adaptive approach [17] would be so required in order to recover the original undeflected trimmed configuration.

Through proper design of the wing-tip device it is possible to increase the wing aspect ratio with little, if any,

increase in the internal loads experienced by the aircraft during a gust, leading to better aerodynamic efficiency and/or reduced structural weight on existing platforms.

Further work is required to improve the characteristics of the hinge device and to develop an experimental prototype.

V.   Acknowledgments

References

[1] Castrichini, A.,Hodigere Siddaramaiah., V., Calderon., D.E., Cooper, J.E., Wilson, T., Lemmens, Y., "Preliminary Investigation of Use of Flexible Folding Wing-Tips for Static and Dynamic Loads Alleviation", *4th RAeS Aircraft Structural Design Conference,* Belfast, 2014.

[2] Khodaparast, H.H, Cooper, J.E., "Rapid Prediction of Worst Case Gust Loads Following Structural Modification", *AIAA Journal*, Vol. 52, No. 2 (2014), pp. 242-254.

[3] Shabana, A., *Dynamics of Multibody Systems*, John Wiley Sons, New York, 1989.

[4] Bampton, M.C.C., Craig, R.R. Jr., "Coupling of substructures for dynamic analyses." AIAA Journal, Vol. 6, No. 7 (1968), pp. 1313-1319.

[5] Canavin, J.R., Likins, P.W., "Floating Reference Frames for Flexible Spacecraft", *Journal of Spacecraft and Rockets*, 14(12):724–732, December 1977.

[6] Agrawal, O.P. , Shabana, A.A., Application Of Deformable-Body Mean Axis To Flexible Multibody System Dynamics, *Computer Methods in Applied Mechanics and Engineering*, Vol. 56, Issue 2, pp.217-245, 1986.

[7] Meirovitch, L., Tuzcu, I., "The Lure of the Mean Axes", Journal of Applied Mechanics*, 74(3), 497-504, 2007.

[8] Albano, E., Rodden, W.P., "A Doublet-Lattice Method for Calculating Lift Distributions on Oscillating Surfaces in Subsonic Flows", *AIAA Journal* v7 n2 1969 pp 279-285.

[9] Rodden, W.P., Johnson, E.H. , *MSC/NASTRAN Aeroelastic Analysis' User's Guide*, MSC Software, USA, 1994.

[10]   Wright, J.R., Cooper, J.E., *Introduction to Aircraft Aeroelasticity and Loads*, John Wiley, 2007.

[11]   Roger, K.L., "Airplane Math Modeling Methods For Active Control Design", *AGARD Structures and Materials Panel*, number CP-228, pp 4-1 - 4-11, AGARD, 1977.

[12]   Waszak, M.R., Buttrill, C.S., Schmidt, D.K., Modeling and Model Simplification of Aeroelastic Vehicles: An Overview, NASA Technical Memorandum 107691, 1992.

[13]   Looye, G., "Integration of rigid and aeroelastic aircraft models using the residualised model method", *International Forum on Aeroelasticity and Structural Dynamics*, number IF-046. CEAS/DLR/AIAAA, 2005.

[14]   Hodigere Siddaramaiah, V., Calderon, D. E., Cooper, J.E., Wilson, T., "Preliminary Studies in the use of Folding Wing-Tips for Loads Alleviation", *Applied Aerodynamics Conference*, Bristol, 2014.

[15]   Tiffany, S.H., Adams, W.R. Jr., "Nonlinear Programming Extensions to Rational Function Approximation Methods for Unsteady Aerodynamic Forces", NASA Technical Paper 2776, 1988.

[16]   Kier, T., "Comparison of Unsteady Aerodynamic Modelling Methodologies with Respect to Flight Loads Analysis", *AIAA Atmospheric Flight Mechanics Conference and Exhibit*, 2005.

[17]   Cooper, J.E., *Adaptive Structures: Engineering Applications*, Wiley, Chichester, England, U.K., 2007, Chap 5.